HHS Public Access

Author manuscript

Biochim Biophys Acta. Author manuscript; available in PMC 2017 October 01.

Published in final edited form as:

Biochim Biophys Acta. 2016 October ; 1860(10): 2157–2168. doi:10.1016/j.bbagen.2016.05.022.

Is There a Relationship between Solubility and Resorbability of Different Calcium Phosphate Phases *in vitro*?

Victoria M. Wu and **Vuk Uskoković**

Advanced Materials and Nanobiotechnology Laboratory, Department of Bioengineering, University of Illinois, Chicago, IL, USA

Abstract

BACKGROUND—Does chemistry govern biology or it is the other way around - that is a broad connotation of the question that this study attempted to answer.

METHOD—Comparison was made between the solubility and osteoclastic resorbability of four fundamentally different monophasic CP powders with monodisperse particle size distributions: alkaline hydroxyapatite (HAP), acidic monetite (DCP), β-calcium pyrophosphate (CPP), and amorphous CP (ACP).

RESULTS—With the exception of CPP, the difference in solubility between different calcium phosphate (CP) phases became neither mitigated nor reversed, but augmented in the resorptive osteoclastic milieu. Thus, DCP, a phase with the highest solubility, was also resorbed more intensely than any other CP phase, whereas HAP, a phase with the lowest solubility, was resorbed least. CPP becomes retained inside the cells for the longest period of time, indicating hindered digestion of only this particular type of CP. Osteoclastogenesis was mildly hindered in the presence of HAP, ACP and DCP, but not in the presence of CPP. The most viable CP powder with respect to the mitochondrial succinic dehydrogenase activity was the one present in natural biological bone tissues: HAP.

CONCLUSION—Chemistry in this case does have a direct effect on biology. Biology neither overrides nor reverses the chemical propensities of inorganics with which it interacts, but rather augments and takes a direct advantage of them.

SIGNIFICANCE—These findings set the fundamental basis for designing the chemical makeup of CP and other biosoluble components of tissue engineering constructs for their most optimal resorption and tissue regeneration response.

Graphical Abstract

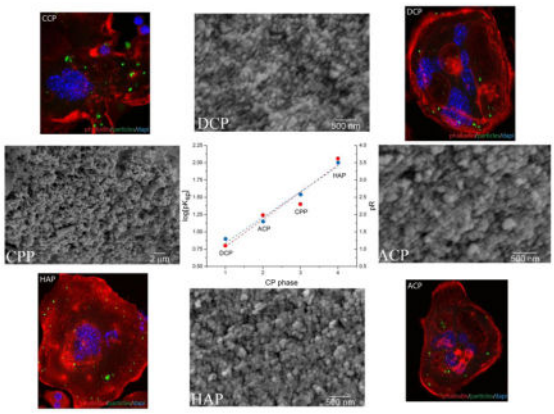

Keywords

Calcium Phosphate; Nanoparticles; RAW264.7; Resorbability; Solubility

Introduction

The field of hard tissue engineering has been preoccupied for a long time by the problem of designing bone replacement materials with the most optimal bioresorption rates. It has been established over time that, ideally, the degradation rate of the bone implant is to match the new bone tissue ingrowth rate. Hydroxyapatite (HAP), the chemically pure version of the mineral component of bone, however, is typified by impractically low resorption rates [1–3]. Reduction of the particle size [4], an increase in porosity [5] and introduction of ionic substitutions, such as magnesium [6], sodium [7], fluorine [8] and/or carbonate [9], so as to mimic the composition and microstructure of biological apatite, have presented approaches to resolving this issue, though with limited success. Namely, even the least sparingly soluble calcium-deficient apatites usually resorb slower than the new bone tissue formation rate [10], whereas HAP with high porosity is weak even to compression and not suitable for load-bearing applications [11]. An alternative approach has comprised admixing more resorbable calcium phosphates, typically tricalcium [12] or dicalcium [13] phosphates, or other calcium compounds, such as sulfates [14] or carbonates [15], to pure HAP.

Calcium phosphates (CPs), in fact, exist in a variety of phase compositions, whose solubility ranges from extremely soluble monocalcium phosphates (MCPs) to moderately soluble dicalcium phosphates (DCPs) to relatively insoluble tricalcium phosphates (TCPs) to sparingly soluble octacalcium phosphate and HAP. The main problem that the use of more resorbable CP phases as bone implants has faced is little control over bioresorption in spite of the known solubility profiles. For example, even though DCP dissolved three times faster than HAP in a solution whose inorganic composition matched that of blood serum [16], implantation of DCP often does not guarantee any faster resorption than implantation of HAP [17–19] This phenomenon supposedly stems from the highly mobile surface layer of charged species common to all CP phases [20]. Constant dissolution and reprecipitation of this layer are expected to take place in solution and in body fluids, leading to an incessant

reorganization of the surface in search of the most stable and chemically equilibrated phase composition for the given chemical conditions of its microenvironment. Thus, for example, after the first burst of dissolution, as a temporary equilibrium is established between the solid surface and the solution, DCP in contact with the body fluid is expected to form a layer of HAP on its surface, which would protect it from further dissolution [21–25]. Being the most stable CP phase at pH > 6.5 [26, 27], HAP is supposed to partially cede place to DCP as an *in vivo* precipitate only under pathological conditions, such as cariogenesis [28], dental calculus formation [29], corneal calcification [30], atherosclerosis [31], calcific arthritis [32], renal and urinary lithiasis [33], osteomyelitis [34], or aggressive osteoporosis [35], or in the zones of excessive osteoclastic activity [36]. Such circumstances are not uncommon, which explains why uncertainties regarding the fate of CP implants in the body are still tied to their use. This is not even to mention the more complex biological processes, ranging from (a) phagocytic to (b) enzymatic degradation to (c) local variations in acidity to (d) more complete wetting of hydrophobic surfaces in biological environments than in aqueous solutions to (e) osteoblastic formation of new bone at the tissue/implant interface as a barrier to osteoclastic access and resorption [37], which could all, individually and in synergy, have an equal say in terms of contributing to deviations of the resorption rates *in vitro* and *in vivo* from the degradation profiles observed in simple solutions [38]. Some CP phases, moreover, do not reach a plateau in the concentration of dissolution units in the supernatant even after 30 days of immersion time [39], suggesting the unusual complexity of the dissolution process. Implant geometry, location of the surgical placement and the identity and composition of cells, proteins and ionic solutes at the implant/tissue interface are all involved in defining the resorption rate of CPs in the body [23]. As a result, the structural transformations conditioning the kinetics of resorption of CP are expected to be complexly dependent on an array of factors other than the simple dissolution propensities of the individual phases in question.

The purpose of this study was to assess the correlation between *in vitro* resorption profiles and solubilities of four different CP phases, ranging from 0.3 to 48 mg/l. Osteoclasts, multinuclear cells whose *in vitro* model, RAW264.7, was used in this study, dissolve the bony tissues by creating a low pH (3 – 4) environment [40] and phagocytosing the mineral particles. They work in precise orchestration with their antagonists, osteoblasts, cells that internally precipitate mineral nanoparticles and deposit them extracellularly, building new bone thereby. As ever, when it comes to proposing correlations between *in vitro* observations and the corresponding patterns present *in vivo*, caution is to be exercised, primarily because osteoclasts are not the only factors that govern the resorption of CPs in the body. Phagocytosis by macrophages is an additional effect that contributes to resorption of bioceramics [38, 41]. The more rapid body fluid flow, reducing the concentration of dissolution units in the near vicinity of the implant, while simultaneously buffering it at a fairly constant level elsewhere, is another factor that greatly affects the resorption rate and is not so readily mimicked under *in vitro* conditions. Coupled to attrition to mimic cyclic mechanical loading, frequent solvent replenishments indeed promoted dissolution of DCP in buffered saline, perhaps by interfering with the protective HAP layer formation at physiological pH [42]. These results have implicitly suggested that different chemical environments and different mechanical loads greatly affect the degradation profile of CP

implants and reiterated the unusual complexity of their fate in the body. Given that their degradation determines the outcome of the bone regeneration and healing process, a broader knowledge of these processes is needed to ensure more reliable, patient- and case-specific orthopedic and dental treatments, which is the niche that the purpose of this work falls in. Although the complexity of degradation pathways present in the body is far more complex than that of the *in vitro* model used in this study, the latter can still offer insights that deepen our knowledge of the degradation of CPs and help us better understand and clinically control its flipside: the regeneration process.

Materials and methods

Synthesis and characterization of different CP nanopowders

The synthesis of different CP powders followed the previously established protocols [43] and involved precipitation from either alkaline or pH-neutral aqueous solutions followed by bringing the precipitate alongside its parent solution to boiling in case of DCP and HAP, as well as annealing at 800 °C for 2 h in air for CPP. The degrees of saturation (DS) were calculated using an algorithm based on Debye-Hückel equation [14]:

$$DS = pK_{sp} - pQ \quad \text{(Eq.1)}$$

$$Q = \{Ca^{2+}\}^{x}\{PO_4^{3-}\}^{y}\{H^{+}\}^{z}\{OH^{-}\}^{w} \quad \text{(Eq.2)}$$

Q is the ionic activity product of the solution, and pK_{sp} is the negative logarithm of the solubility product of a given CP phase (Table 1). Activity coefficients were calculated through $\log\gamma = -Az_i^2 I^{1/2}$, where z_i is the charge number of ion species i, I is the ionic strength of the solution, and A is the-temperature dependent constant equal to 0.5115 at 25 °C. B and a_i are, like A, constants depending on temperature, dielectric constant of the solution and Debye screening length; a_i = 6 x 10^{-8} for Ca^{2+}; 9 x 10^{-8} for H^+; and 4 x 10^{-8} for $H_xPO_4^{x-3}$/$CaH_{2x}PO_4^{2x-1}$. Appropriate dissociation constants for H_2O and $H_xPO_4^{x-3}$ and association constants for $CaH_xPO_4^{x-1}$, $CaH_xCO_3^{x}$ and Ca---OH were taken into account as functions of pH [44].

X-ray diffraction (XRD) studies were carried out on a *Siemens* D500 diffractometer using $Cu_{K\alpha}$ = 1.5418 Å as the wavelength of the radiation source. The average size of the crystallites was determined using a structural refinement approach (Topas 2.0) based on the previously identified crystal structure (PCPDFWIN & Eva) and taking the instrumental broadening into account. The morphology of the powders was analyzed on a *Hitachi* S-4300SE/N scanning electron microscope (SEM) at the electron beam energy of 15 kV.

Cell culture

Mouse monocyte macrophage RAW264.7 cells were obtained from *ATCC* and cultured in Dulbecco's modified Eagle medium (DMEM) with 10 vol% fetal bovine serum and 5 vol% amphotericinB (streptomycin/penicillin/fungisone) as the antibiotic/antimycotic. To

differentiate them into an osteoclast-like phenotype, they were seeded at 1.5 x 10^5 cells/well in 24 well plates and incubated for 7 – 9 days in the medium additionally containing 35ng/ml RANKL/TRANCE (*R&D system*). The medium was replaced every other day and differentiated, large multinucleated cells could be seen in the wells by Day 5. On Day 7, the cells were stained for Tartrate-resistant acid phosphatase (TRAP) using a commercial acid phosphatase leucocyte kit (*Sigma*). Images were obtained using an Olympus BX51 microscope (UIC core imaging facility).

Real Time qPCR

Total RNA was extracted from cells using the RNeasy kit (Qiagen) and cDNA synthesized using the High-Capacity cDNA reverse transcription kit (Applied Biosystems) from 100 ng of total RNA. cDNA was quantified using custom TaqMan probes for cathepsin K (CTSK) Mm00484039_m1, Acp5 (TRAP) Mm00475698_m1, Tnfsf11 (RANKL) Mm00441906_m1 and Polymerase (RNA) II (Polr2a) Mm00839502_m1 on a StepOne Real Time PCR System (Applied Biosystems). Analysis of housekeeping genes was done using the mouse endogenous control plate from Life Technologies. The real-time PCR results were analyzed using the $\Delta\Delta C_t$ method and all the data were normalized to Polr2a expression levels. All the samples were analyzed in three experimental triplicates and three analytical replicates (n = 3 x 3 = 9).

Immunohistochemistry

RAW264.7 cells seeded at 5.5 x 10^5 cells/well in 24-well plates and differentiated for 7 days in media containing 5 mg/well of CP nanoparticles. Cells on coverslips were then first washed with 1x PBS to remove the nanoparticles that had not been endocytosed, then fixed for 5 minutes in 4 wt% paraformaldehyde, then washed with 1x PBS and incubated with Alexa Fluor 568 Phalloidin (1:400) (*Molecular Probes*) and OsteoImage™ bone mineralization staining agent (*Lonza*) for 30 minutes (for HAP, DCP and ACP) and 1 hour (for CPP), according to the protocol described by *Lonza*. After incubation, coverslips were rinsed in 1x PBS and washed for 3 x 5 minutes in 1x PBS. Cell nuclei were then counterstained using NucBlue fixed cell ReadyProbe reagent (*Molecular Probes*) for 20 minutes. Images were acquired on a Zeiss LSM 710 confocal microscope (UIC core imaging facility).

MTT cell viability assay

RAW264.7 cells were seeded at 5.5 x 10^5 cells/well in 24-well plates and differentiated for 7 days with 35ng/ml of mRANKL in the presence of 5 mg/well of HAP, DCP, ACP or CPP nanoparticles. Cell viability was then determined using the Vybrant MTT cell proliferation assay (*Molecular Probes*). All the samples were analyzed in triplicates and compared against two types of controls treated under identical conditions, one of which contained mRANKL-treated RAW264.7 cells with no CP particles, and the other one of which contained only the cell culture medium.

Cell differentiation assay

RAW264.7 cells were seeded at 5.5 x 10^5 cells/well in 24-well plates and differentiated for 7 days with 35ng/ml of mRANKL in the presence of 5 mg/well of HAP, DCP, ACP or CPP nanoparticles. The number of cells containing five or more nuclei was then counted on each cover slip under a Nikon T1-S/L100 inverted epifluorescent optical microscope. All the samples were analyzed in triplicates and compared against the control samples treated under identical conditions and containing mRANKl-treated RAW264.7 cells with no CP particles.

Calcium ion release assay

RAW264.7 cells were seeded at 5.5 x 10^5 cells/well in 24-well plates and differentiated for 9 days with 35ng/ml of mRANKL in the presence of 5 mg/well of HAP, DCP, ACP or CPP and 1 ml of DMEM per well. The media in which the cells were cultured with the CP nanoparticles were removed at days 2, 5, 7 and 9 and free Ca^{2+} ion concentration levels in the media for each of the days were measured using the Ca^{2+} microelectrode in combination with a reference electrode (*Microelectrodes, Inc.*) on an Accumet AB250 pH-meter (*Fisher Scientific*). The same experiment, labeled as control, using identical incubation conditions, was carried out in the absence of the cells. Linear calibration curve was created using 0.1 – 5 mM $CaCl_2$ solutions in the same aqueous medium in which the resorption assay was conducted. All the samples were analyzed in triplicates and compared against the control samples containing no cells, only CP particles suspended in the cell culture medium.

Fluorescence measurement of labeled CP nanoparticles

RAW264.7 cells were seeded at 5.5 x 10^5 cells/well in 24-well plates and differentiated for 14 days with 35ng/ml of mRANKL and 5 mg/well of OsteoImage™-labeled HAP, ACP, DCP or CPP nanoparticles. The nanoparticles were fluorescently labeled for 2 hours at room temperature by following the OsteoImage™ bone mineralization assay protocol. Fluorescence levels of labeled particles were assessed at days 0, 1, 2, 5, 7, 9, 11 and 14 using a FLUOstar Omega plate reader (*BMG Labtech*). The excitation and detection wavelengths were 492 and 520 nm, respectively. All the samples were analyzed in triplicates and compared against the control samples containing no cells, only CP particles suspended in the cell culture medium.

Results and discussion

Four different monophasic CP powders were synthesized for the purpose of this study: hydroxyapatite (HAP), dicalcium phosphate anhydrous a.k.a. monetite (DCP), β-calcium pyrophosphate (CPP), and amorphous calcium phosphate (ACP). This selection is justified by our intention to cover the broadest possible spectrum of chemical compositions of CPs, given that each of these CPs is fundamentally chemically different from all the others. Thus, HAP is the only alkaline CP out of all these four powders and the only one present in healthy mammalian bone tissues; DCP is the only acidic one among them, strictly found in pathogenic calcified tissues; CPP is the only CP that is a pyrophosphate, not an orthophosphate, having $P_2O_7^{4-}$ group instead of the $H_xPO_4^{x-3}$ one; and ACP is the only amorphous phase among them. Their chemical formulas and crystallographic symmetries, along with solubility products and solubility values under standard conditions, are given in

Table 1. There is approximately an order of magnitude difference in solubility between the chosen CPs, with the exception of the difference between DCP and CPP. DCP is the most soluble of them, followed by CPP, ACP and HAP, the least soluble CP (not counting for ion-substituted fluoroapatite). The reasonable separation of their solubilities and solubility products is illustrated in Fig. 1, where $\log(pK_{sp})$ ($R^2 = 0.93$) and p function of solubility ($R^2 = 0.98$) are linearly fitted as a function of the number of the four different CP phases.

The particles of HAP, ACP and DCP had sizes in the 50 – 150 nm range (Fig. 2). Due to annealing, CPP particles were larger, having 300 nm in size on average. The boiling step was crucial in terms of preventing DCP from adopting the characteristic, plate-shaped microparticle form and allowing it to precipitate as monodisperse spherical nanoparticles [45]. All the particles were spherical and their size distribution was equally narrow. The similarity in particle size and shape across different CP phases is an important prerequisite for the reliable comparison of their chemistries. This is particularly so because solubility is inversely proportional to the particle size [46] and because a difference in the size of CP particles [47] or aggregates [48] can produce a difference in the osteoclastic cell response. Also, all the particles were submicron in size, similar to the CP particles comprising all hard tissues in the human body, from dentin to enamel to bone. Such comparatively small particle size facilitates resorption and bone remodeling [49], the process in which osteoclasts play a central role.

X-ray diffractograms of different CP phases confirm their monophasic compositions (Fig. 3). They also confirm the amorphous nature of ACP as well as that the crystallite sizes are in the nanometer range for HAP (12 nm), DCP (33 nm) and even for the annealed CPP (16 nm). The diffraction profile of DCP matches that of the anhydrous phase, a.k.a. monetite, which forms through dehydration of the brushite lattice during boiling. The diffractogram of CPP corresponds to the low temperature, β modification, as the result of thermal processing at 800 °C, which is higher than 740 °C as the upper range of temperatures at which $\gamma \rightarrow \beta$ transition occurs and also significantly lower than the 1171 – 1179 °C range in which the transition to the α polymorph has been documented to occur [50].

The results of TRAP staining demonstrate the RANKL-mediated transformation of RAW264.7 cells into macrophage-like, multinucleated giant cells, which are osteoclastic in nature (Fig. 4a). Morphologically, the cells are also visibly typified by the invaginated ruffled membrane, which favors an intense resorptive activity by making a greater surface area available for endocytosis and for the secretion of protons and digestive enzymes. In addition, cells were assessed for the regulation of a number of differentiation markers typical for the osteoclast phenotype (Fig. 4b). Prior to that, a detailed analysis of the activity of housekeeping genes in RAW264.7 cells was conducted in search of the most optimal internal control. As could be seen from Fig. 3b, although 18S rRNA, glyceraldehyde-3-phosphate dehydrogenase (GAPDH) and β-actin (ACTB) are typical choices for such controls, their expression is far from optimal, peaking at C_t values of 9.1, 19.4 and 21.0, respectively, and also being associated with comparatively high standard deviations (SDs) of 0.4, 0.1 and 0.4, respectively. Ubiquitin C (UBC), another frequent choice, demonstrates very low SD of 0.01, but its C_t of 21.48 is lower than the optimal C_t range of 23 to 27. For that reason, our choice has settled on polymerase (RNA) II polypeptide A (PolR2a), the

second closest gene to $C_t = 25$, having $C_t = 24.485$, and the one with the highest uniformity of expression among all the eight genes falling within $23 < C_t < 27$, having the SD of 0.046. To determine that RAW 264.7 cells did indeed differentiate into an osteoclastic cell type, real-time qPCR was used to measure the expression levels of two different markers of osteoclast differentiation, cathepsin K (CTSK) and Acp5 (TRAP) [55]. Analysis of CTSK and TRAP, Fig. 3c, showed that the expression of both osteoclast markers was upregulated. In contrast, the expression of the markers of osteoblast differentiation, RANKL and Runx2, was at a barely detectable level. Both the gene expression analysis and the morphological analysis of the RANKL-treated RAW264.7 cells using TRAP staining thus demonstrated that the cells were successfully and correctly differentiated into an osteoclastic cell type.

Immunohistochemistry analyses were performed to visualize the uptake of fluorescently labeled CP particles and gain an insight into their effect on the cell number, multinucleation and morphology. As seen from Fig. 5b–e, all the four different types of CP particles were successfully uptaken by the osteoclastic cells, without producing any adverse effects. No morphological difference was evidenced for osteoclastic cells during or following the particle uptake when compared to the particle-free control (Fig. 5a), suggesting the overall positive effect of CP particles on this cell population. Looking at the particle retention following the uptake, however, it is apparent that CPP becomes retained inside the cells for the longest period of time, indicating hindered digestion of only this particular type of CP (Fig. 5f).

Most prior studies on osteoclastic resorption were qualitative and methodologically unsuitable for delineating fine differences between the resorptive propensities of different materials. In this study we developed a new model for the estimation of resorbability based on measuring a time-dependent drop in photoluminescence of fluorescently stained particles *in vitro*. The results of measuring the decrease in fluorescence of CP particles labeled with the fluorescent agent OsteoImage™ are shown in Fig. 6. The decrease in fluorescence is assumed to correspond to the progression of the particle degradation process, not accounting for desorption of the fluorophore, which was assumed to be the same for all the particle types incubated under identical conditions. The lowest resorption and solubility were observed for HAP and the highest ones for DCP (Fig. 6a–b), which is in agreement with their chemical propensities for dissolution. For CP powders in aqueous solution on the final day of the measurement (day 14), the same trend as expected from the prior empirical data (Table 1) was observed, with the solubility following this trend: DCP > CPP > ACP > HAP (Fig. 6b). At the same time point of the analysis in cell culture, this trend was inverted only insofar as the solubility of CPP happened to be lower than any of the other three CP phases, which continued to follow the trend concordant with the expected: DCP > ACP > HAP (Fig. 6a).

As expected, the degradation of all CP powders was intensified in the presence of osteoclasts (Fig. 6c–f). The least of the difference was seen for the least soluble CP, HAP, in which case only initially and after 7 days of incubation did the two curves, one representing cellular and other representing acellular conditions, diverge (Fig. 6c). In turn, the largest difference in degradation between aqueous and osteoclastic environments was observed for DCP (Fig. 6d), suggesting that cells do have the ability to augment the intrinsic propensity for

dissolution of this particular CP phase. The difference in the degradation profiles between different CP phases in the acellular milieu becomes expanded in the osteoclastic environment.

Calcium ion release experiments corroborate the lowest resorption and solubility observed for HAP and the highest ones for DCP. DMEM as the cell culture medium, having $[Ca^{2+}]$ = 1.8 mM, $[H_xPO_4^{x-3}]$ = 0.9 mM, $[H_xCO_3^{x-2}]$ = 44 mM and the background ionic strength of 150 mM, is supersaturated with respect to HAP (DS = 9.7 at 37 °C), as opposed to being undersaturated with respect to DCP (DS = − 0.6) and ACP (DS = − 2.1). For this reason, HAP and ACP particles suspended in this medium act as crystallization nuclei and free Ca^{2+}, $H_xPO_4^{x-3}$ and OH^- ions in the buffered medium become reprecipitated to some extent on their surface. This explains the lower free Ca^{2+} levels in the supernatant for these two systems when compared to the particle-free control (Fig. 7a–b). In fact, even though DMEM has lower $[Ca^{2+}]$ and $[H_xPO_4^{x-3}]$ than Kokubo's SBF [56] (1.8 vs. 2.5 mM and 0.9 vs. 1.0 mM, respectively), which has been routinely used for *in vitro* bioactivity tests, ACP was spontaneously precipitated from it on the surface of a 45S5 glass-ceramic scaffold [57, 58]. ACP is additionally typified by the flexible surface prone to rearrange its structure in the direction of adopting one even more resistant to dissolution than the lowly crystalline HAP. This volatile compositional nature of ACP is illustrated by the linear increase of the degradation rate over the course of the experiment, contrasting the steady degradation rate of HAP in the same period of time (Fig. 7a). Moreover, following prolonged aging in alkaline solutions, ACP tends to partially transform to HAP stoichiometry. We have consistently observed the induction of this phase transformation by prolonged aging under ambient conditions, the reason for which the method of synthesis of ACP involved abrupt precipitation, sedimentation and desiccation. This explains little difference between HAP and ACP in terms of their dissolution estimated by Ca^{2+} release experiments in the osteoclastic culture at the final time point of incubation. In contrast, because of its intrinsic acidity, DCP dissolves in the basic media and $[Ca^{2+}]$ becomes higher than that of the medium *per se* (Fig. 7b). The most intense increase in $[Ca^{2+}]$ in the osteoclastic milieu was observed exactly for DCP, a CP stoichiometry with the highest K_{sp} among those analyzed here. A similar increase in $[Ca^{2+}]$ in the osteoclastic cell culture compared to the regular solution was recently observed for monetite, the DCP phase utilized in this study [59]. The same effect is observed here for CPP, though only in the presence of the osteoclastic cells; in their absence, no degradation of this stoichiometry occurred, as indicated by the overlap of Ca^{2+} release curves for CPP and the control medium (Fig. 7b). In the absence of pyrophosphate groups and free protons in the alkaline medium, DCP and CPP cannot be reprecipitated and they cannot drag the released Ca^{2+} back to the solid phase, as observed for ACP and HAP, which explains the higher levels of Ca^{2+} than that of the control medium in their supernatants. In fact, similar to their structural analogs, bisphosphonates [60, 61], pyrophosphate ions have been known for a long time to be equally strong endogenous inhibitors of precipitation of any calcium orthophosphates [62, 63], including DCP and HAP. Moreover, stabilization of $[Ca^{2+}]$ at identical values following each solvent replacement under the control, osteoclast-free conditions unequivocally indicates a saturation-driven degradation, which is, as such, directly controllable by the solubility product. The fact that the same trend is observed in the presence of osteoclasts for all three orthophosphate

compositions suggests that the resorption is in their case also controlled by the solubility product. All in all, conforming to the results of the fluorescence test, [Ca^{2+}] release experiments demonstrate that the increase in the degradation rate in the osteoclastic environment is directly proportional to the solubility of CP powders in regular solutions, having obeyed the following trend: DCP > CPP > HAP > ACP. ACP was the only phase that differed in response in these two comparative analyses, eliciting a relatively abundant release of the staining agent and a low release of Ca^{2+} ions. This can be explained by its being a CP phase capable of high drug loading and release despite moderate degradation rate, which is an effect attributable to its amorphous and transient, high-energy surface structure.

CPP was typified by a relatively low degradation rate based on fluorescence measurements and a relatively high Ca^{2+} ion release rate. Although this may initially seem contradictory, the explanation of this discrepancy is obvious: namely, whereas Ca^{2+} ions are easily stripped off the endocytosed CPP particles, the cells have a more difficult time degrading the network of pyrophosphate ions, which are also bulkier and less hydratable than phosphates. The first step in the hydration of CPP involves the weak binding of water molecules to Ca^{2+} ions and the breaking of the bonds between pyrophosphate and Ca^{2+} [64], yielding a layered structure similar to that typifying DCPs [65]. The release of Ca^{2+} and the hydrolysis of pyrophosphate are the two main mechanisms for dissolution of CPPs, with the former tending to proceed more favorably than the latter, judging based on the relatively large Ca---O bond lengths (and their inverse proportionality to the bond strength)[66], the short distance between oxygen atoms of the two phosphates in the eclipsed pyrophosphate configuration and other parameters of the crystallographic order of β-CPP [67]. The timescale for hydrolysis of pyrophosphate to phosphate in neutral aqueous solutions is in the order of decades [68] and is facilitated by phagocytosis and the presence of enzymes, e.g. alkaline phosphatase [69], or other proteins, e.g. albumin [51], under physiological conditions. This is demonstrated by [Ca^{2+}] experiment where the release of Ca^{2+} from CPP particles was observed strictly in the presence of the osteoclastic cells (Fig. 7f), whereas [Ca^{2+}] values were identical to the cell culture medium in their absence throughout the entire course of the experiment (Fig. 7b). As demonstrated in Fig. 5, CPP particles occupied the largest percentage of the interior of differentiated, osteoclastic RAW264.7 cells, suggesting their extensive uptake, but inhibited resorption. The robustness of pathological deposits of CPP in the body and their resistance to degradation have been documented earlier [70]. Finally, the inhibitory effect CPP particles had on the osteoclastic resorption is equivalent to that exhibited by their structural analogs, bisphosphonates, which reverse the symptoms of osteoporosis not by inducing new bone formation, but by inhibiting the osteoclastic activity [71, 72].

The number of differentiated cells, that is, cells with five or more nuclei per surface area was significantly ($p < 0.05$) lower compared to the control for all CP powders except CPP (Fig. 8a). The reason may be that CPP, as the only pyrophosphate, is recognized as the most chemically foreign solid out of all these phases. As such, it may elicit the most rapid differentiation response from this essentially immune cell lineage, which is metabolically activated by foreign bodies more than by the host biomolecular species. Namely, unlike osteoblasts, which are derived from mesenchymal stem cells, osteoclasts are derived from the same $CD14^{+}$ hematopoietic stem cells from which monocytes, macrophages and dendritic cells originate [73]. Given their derivation from bone marrow and phagocytic,

multinuclear nature, they are often considered as specialized blood cells, akin to macrophages, rather than true bone cells, which may explain their metabolic activation, not suppression, by the presence of foreign species. Now, although pyrophosphate, a product of the conversion of adenosine triphosphate to adenosine monophosphate, is a less common ion in the body compared to the phosphate, it was still detected in extraosseous calcific deposits [74–76], while its proposed role in the regulation of bone remodeling has been on hold for many years now [77]. Finally, although CPP has been shown to induce the apoptosis of osteoclasts [78] and induce an intense inflammatory response [79–81], no *in vitro* hints of such effects were observed in this study. Also, although bisphosphonates as structural analogs of pyrophosphates inhibit the resorption of bone by inducing the apoptosis of osteoclasts, aside from the inhibited resorption of CPP we observed no markedly adverse effects on the interaction between the CP particles and the osteoclastic cells. Finally, osteoclastogenesis appears to have been hindered in the presence of HAP, ACP and DCP, but considering the particle concentration of 2.6 mg/ml the observed effect was nowhere as pronounced as the 3- to 300-fold reduction in the number of differentiated osteoclastic cells following incubation with different metallic particles (Ti, FeTiCr, CoCr28Mo6 and TiAl6Nb7) at the concentration of only 1 mg/ml [82].

In our previous study we have shown that the combination of (a) a pronounced acidic nature of a CP powder and (b) its high solubility can be lethal for cultured cells. Thus, MCP powders proved to be cytotoxic under conditions of impeded medium flow [45]. In contrast, the stoichiometric acidity of DCP powders ($CaHPO_4$) is four times lesser than that of MCP ($Ca(H_2PO_4)_2$). Their solubility is also by three orders of magnitude lower than that of MCP (17 vs. 0.05 g/l under standard conditions for anhydrous phases). As such, they do not reduce cell viability when added in moderate amounts. At 2.6 mg/cm^2, though, viability was reduced down to 20 % of that of the particle-free control (Fig. 8b). Naturally, the most viable CP powder with respect to the mitochondrial succinic dehydrogenase activity that the MTT assay responds to was the one present in biological bone tissues: HAP. Its addition to osteoclastic cells increased their viability by 20 %. There was no statistically significant difference in viability of cells incubated with ACP and CPP when compared to the negative, particle-free control.

Summary and outlook

With the fate of biodegradable bone replacement materials being greatly determined by their ability to degrade at the exact rate at which the new tissue replaces them, understanding the kinetics of resorption of CPs, so frequently used for this application, is of utmost importance. Although the emphasis of hard tissue engineers is currently mostly on augmentation of bone growth, the control of the antagonistic process of bone resorption, which keeps its complement in check, is of equally pivotal importance. For, without controlled osteolysis, bone would have no ability to repair itself and be remodeled under the demands of its bio-physicochemical microenvironment [83]. Although osteoclast inhibition with bisphosphonate treatments, serving the purpose of reducing bone loss due to stress-shielding effect, has improved the postoperative outcome of bone replacement procedures, a complete suppression of the osteoclast activity would make the stable bone/implant union impossible. The osteoclastic resorption of bone also releases and activates TGF-βs, which

initiate a cascade of responses to injury in nearby cells, implying that no fracture healing could occur without osteolysis [84]. Other problems, such as hypocalcemia resulting from the inability to utilize calcium reposited in the bone or failure under cyclic loading would also be immanent in the absence of osteoclasts. Thus, although osteoblasts have been traditionally considered as the key mediators of the osseointegration process, osteoclasts are equally important determinants of the fate of bone replacement materials in the body [85], regardless of whether they are bioresorbable or not. The ability of a material to be resorbed by osteoclasts, consequently, need not be a sign of its adversity, but quite the opposite, given that autologous bone, the gold standard in the bone replacement domain, is resorbed unprecedentedly well owing to its unique microstructure and composition.

This study looked at the effect of different CP chemistries on their resorption by an osteoclastic RAW264.7 cell line. Our motivation for *in vitro* tests owes to the fact that, unlike *in vivo* analyses, they are capable of differing between the physicochemical and cellular degradation, which was exactly the objective of this study. Resorption was quantified by measuring (a) the calcium ion release into the cell culture medium, (b) the reduction in luminescence of fluorescently tagged CP nanoparticles over up to two weeks of incubation time, and (c) the cross-sectional surface coverage of the cytoplasmic interiors of osteoclastic cells by the fluorescently stained CP nanoparticles. The same methods, with the exception of (c), were used to assess the solubility of CP particles in the absence of the cells. By comparing the degradation profiles between these two modes, we have come to conclusion that chemical propensities of CP powders are the determinants of their osteoclastic resorbability. The difference in solubility between these CP phases becomes neither mitigated, annulled nor reversed, but rather augmented in the resorptive osteoclastic milieu. Based on solubility values in aqueous solutions one would expect HAP to degrade slower than any of the four CP phases tested in parallel in this work, and this was exactly the case: HAP was the phase resorbed less intensely than DCP, CPP or ACP. The following trend in solubility, DCP > ACP > HAP, remained in effect in the osteoclastic cell culture. With rare exceptions [86], the literature data are in agreement with these findings, at least concerning the biphasic CP cements: namely, TCP, otherwise more soluble phase than HAP, has been consistently more rapidly degraded by osteoclasts *in vitro* than HAP [87, 88]. In spite of the expectation that osteoclasts might degrade DCP slower than HAP because DCP is a more stable phase than HAP at pH < 4.2 [89], the opposite effect, conforming to the solubility trends under physiological conditions (pH > 7), was evidenced in this study. It is uncertain what cellular mechanisms osteoclast utilize to exhibit this solubility augmentation effect. Acidification of the solution has an increasing effect on the solubility of all CP phases below the minimum at pH 8 – 9 depending on the phase [90], and it is possible that the acidic endosome facilitates the degradation of CPs in direct proportion with their solubility under standard conditions. CPP was the only CP phase whose dissolution was obstructed following the particle uptake. It appears that CPP as a pyrophosphate provided the cells with a form of phosphate less readily resorbable than that of the orthophosphate. Its effect on the osteoclastic cells appears analogous to that of its structural analogs, bisphosphonates, which inhibit the osteoclastic resorption and are used, as such, to fight osteoporosis. Finally, if we were to go back to the question with which this report opened - does chemistry govern biology or it is the other way around – the answer would be that chemistry does have an

effect on biology, though with exceptions exemplified by the CPP phase. At least when the orthophosphates are in question, the empirical solubility profiles valid for regular aqueous solutions apply well for the resorption conditions. To that effect, there is a definite relationship between the solubility and resorbability of a set of calcium orthophosphate phases *in vitro* and under the experimental conditions utilized in this study.

All the CP phases were uptaken by the osteoclastic cells and no negative morphological indications were observed in the cells during or following the digestion of the CP powders. Aside from the lowered viability caused by the intrinsically acidic DCP, all powders elicited a positive response from the osteoclastic cells. From the perspective of application in bone regeneration, the results obtained here do not discredit any of the CP phases. Still, given the moderate, but definite demerits of all individual CPs, ranging from the low biodegradation profile of HAP to pronounced acidity and considerably faster degradation of DCP, it is perhaps their combination that offers most potential benefits in substituting and/or regenerating impaired hard tissues. By controlling the bone substitute degradation process using various CP phases, broader in composition that the combination of HAP and β-TCP that is usually applied in biphasic bone cements, resorption could be tailored to favor bone regeneration. For example, as implied by the findings of this study, HAP content could be increased where bone ingrowth is slow and where osteoconduction is favored; ACP content could be increased when bone remodeling is also relatively slow, but a faster release of the adsorbed drug is intended; DCP contents could be increased where quicker degradation is desired; and CPP content could be increased where osteoclastic resorption is to be hindered. This study attempts to provide the basis for future, more detailed studies in the direction of the design of such, more structurally complex bone replacement materials.

Acknowledgments

NIH grant R00-DE021416 is acknowledged for support.

References

1. Klein CP, Driessen AA, de Groot K, van den Hooff A. Biodegradation behavior of various calcium phosphate materials in bone tissue. J Biomed Mater Res. 1983; 17:769–784. [PubMed: 6311838]
2. Okuda T, Ioku K, Yonezawa I, Minagi H, Gonda Y, Kawachi G, Kamitakahara M, Shibata Y, Murayama H, Kurosawa H, Ikeda T. The slow resorption with replacement by bone of a hydrothermally synthesized pure calcium-deficient hydroxyapatite. Biomaterials. 2008; 29:2719–2728. [PubMed: 18403011]
3. Von Rechenberg B, Genot OR, Nuss K, Galuppo L, Fulmer M, Jacobson E, Kronen P, Zlinszky K, Auer JA. Evaluation of four biodegradable, injectable bone cements in an experimental drill hole model in sheep. Eur J Pharm Biopharm. 2013; 85:130–138. [PubMed: 23680585]
4. Detsch R, Hagmeyer D, Neumann M, Schaefer S, Vortkamp A, Wuelling M, Ziegler G, Epple M. The resorption of nanocrystalline calcium phosphates by osteoclast-like cells. Acta Biomater. 2010; 6:3223–3233. [PubMed: 20206720]
5. Okanoue Y, Ikeuchi M, Takemasa R, Tani T, Matsumoto T, Sakamoto M, Nakasu M. Comparison of in vivo bioactivity and compressive strength of a novel superporous hydroxyapatite with beta-tricalcium phosphates. Arch Orthop Trauma Surg. 2012; 132:1603–1610. [PubMed: 22760581]
6. Roy M, Bose S. Osteoclastogenesis and osteoclastic resorption of tricalcium phosphate: effect of strontium and magnesium doping. J Biomed Mater Res A. 2012; 100:2450–2461. [PubMed: 22566212]

7. Sang Cho J, Um SH, Su Yoo D, Chung YC, Hye Chung S, Lee JC, Rhee SH. Enhanced osteoconductivity of sodium-substituted hydroxyapatite by system instability. J Biomed Mater Res B Appl Biomater. 2014; 102:1046–1062. [PubMed: 24307519]
8. Kannan S, Rocha JH, Agathopoulos S, Ferreira JM. Fluorine-substituted hydroxyapatite scaffolds hydrothermally grown from aragonitic cuttlefish bones. Acta Biomater. 2007; 3:243–249. [PubMed: 17127113]
9. Spence G, Patel N, Brooks R, Bonfield W, Rushton N. Osteoclastogenesis on hydroxyapatite ceramics: the effect of carbonate substitution. J Biomed Mater Res A. 2010; 92:1292–1300. [PubMed: 19343778]
10. Chissov VI, Sviridova IK, Sergeeva NS, Frank GA, Kirsanova VA, Achmedova SA, Reshetov IV, Filjushin MM, Barinov SM, Fadeeva IV, Komlev VS. Study of in vivo biocompatibility and dynamics of replacement of rat shin defect with porous granulated bioceramic materials. Bull Exp Biol Med. 2008; 146:139–143. [PubMed: 19145372]
11. Sun F, Zhou H, Lee J. Various preparation methods of highly porous hydroxyapatite/polymer nanoscale biocomposites for bone regeneration. Acta Biomater. 2011; 7:3813–3828. [PubMed: 21784182]
12. Daculsi G, LeGeros RZ, Nery E, Lynch K, Kerebel B. Transformation of biphasic calcium phosphate ceramics in vivo: ultrastructural and physicochemical characterization. J Biomed Mater Res. 1989; 23:883–894. [PubMed: 2777831]
13. Ko CL, Chen JC, Tien YC, Hung CC, Wang JC, Chen WC. Osteoregenerative capacities of dicalcium phosphate-rich calcium phosphate bone cement. J Biomed Mater Res A. 2015; 103:203–210. [PubMed: 24639027]
14. Nilsson M, Zheng MH, Tagil M. The composite of hydroxyapatite and calcium sulphate: a review of preclinical evaluation and clinical applications. Expert Rev Med Devices. 2013; 10:675–684. [PubMed: 24053255]
15. Jamali A, Hilpert A, Debes J, Afshar P, Rahban S, Holmes R. Hydroxyapatite/calcium carbonate (HA/CC) vs. plaster of Paris: a histomorphometric and radiographic study in a rabbit tibial defect model. Calcif Tissue Int. 2002; 71:172–178. [PubMed: 12200649]
16. Chow LC, Markovic M, Takagi S. A dual constant-composition titration system as an in vitro resorption model for comparing dissolution rates of calcium phosphate biomaterials. J Biomed Mater Res B Appl Biomater. 2003; 65:245–251. [PubMed: 12687717]
17. Bohner M, Theiss F, Apelt D, Hirsiger W, Houriet R, Rizzoli G, Gnos E, Frei C, Auer JA, von Rechenberg B. Compositional changes of a dicalcium phosphate dihydrate cement after implantation in sheep. Biomaterials. 2003; 24:3463–3474. [PubMed: 12809775]
18. Penel G, Leroy N, Van Landuyt P, Flautre B, Hardouin P, Lemaitre J, Leroy G. Raman microspectrometry studies of brushite cement: in vivo evolution in a sheep model. Bone. 1999; 25:81S–84S. [PubMed: 10458282]
19. Jiang W, Chu X, Wang B, Pan H, Xu X, Tang R. Biomimetically triggered inorganic crystal transformation by biomolecules: a new understanding of biomineralization. J Phys Chem B. 2009; 113:10838–10844. [PubMed: 19591436]
20. Uskokovic V. Nanostructured platforms for the sustained and local delivery of antibiotics in the treatment of osteomyelitis. Crit Rev Ther Drug Carrier Syst. 2015; 32:1–59. [PubMed: 25746204]
21. Driessens FC. Physiology of hard tissues in comparison with the solubility of synthetic calcium phosphates. Ann N Y Acad Sci. 1988; 523:131–136. [PubMed: 3289449]
22. Driessens, VRFCM. Implant materials in biofunction. Elsevier; Amsterdam: 1988.
23. Grover LM, Knowles JC, Fleming GJ, Barralet JE. In vitro ageing of brushite calcium phosphate cement. Biomaterials. 2003; 24:4133–4141. [PubMed: 12853243]
24. Constantz BR, Barr BM, Ison IC, Fulmer MT, Baker J, McKinney L, Goodman SB, Gunasekaren S, Delaney DC, Ross J, Poser RD. Histological, chemical, and crystallographic analysis of four calcium phosphate cements in different rabbit osseous sites. J Biomed Mater Res. 1998; 43:451–461. [PubMed: 9855204]
25. Tas AC, Bhaduri SB. Chemical Processing of CaHPO42H2O: Its Conversion to Hydroxyapatite. J Am Ceram Soc. 2004; 87:2195–2200.

26. Strates BS, Neuman WF, Levinskas GJ. The solubility of bone mineral. II. Precipitation of near neutral solutions of calcium and phosphate. J Phys Chem B. 1957; 61:279–282.
27. Kaufman HW, Kleinberg I. An X=ray crystallographic examination of calcium phosphate formation in Ca(OH)2/H3PO4 mixtures. Calc Tissue Res. 1971; 6:335–342.
28. Shellis RP, Heywood BR, Wahab FK. Formation of brushite, monetite and whitlockite during equilibration of human enamel with acid solutions at 37 degrees C. Caries Res. 1997; 31:71–77. [PubMed: 8955998]
29. Jin Y, Yip HK. Supragingival calculus: formation and control. Crit Rev Oral Biol Med. 2002; 13:426–441. [PubMed: 12393761]
30. Huige WM, Beekhuis WH, Rijneveld WJ, Schrage N, Remeijer L. Deposits in the superficial corneal stroma after combined topical corticosteroid and beta-blocking medication. Eur J Ophthalmol. 1991; 1:198–199. [PubMed: 1821214]
31. Olsson LF, Odselius R, Ribbe E, Hegbrant J. Evidence of calcium phosphate depositions in stenotic arteriovenous fistulas. Am J Kidney Dis. 2001; 38:377–383. [PubMed: 11479165]
32. Hamada J, Tamai K, Ono W, Saotome K. Does the nature of deposited basic calcium phosphate crystals determine clinical course in calcific periarthritis of the shoulder? J Rheumatol. 2006; 33:326–332. [PubMed: 16465665]
33. Gnessin E, Mandeville JA, Handa SE, Lingeman JE. Changing composition of renal calculi in patients with musculoskeletal anomalies. J Endourol. 2011; 25:1519–1523. [PubMed: 21810030]
34. Esmonde-White KA, Esmonde-White FW, Holmes CM, Morris MD, Roessler BJ. Alterations to bone mineral composition as an early indication of osteomyelitis in the diabetic foot. Diabetes Care. 2013; 36:3652–3654. [PubMed: 23920085]
35. Sogaard CH, Mosekilde L, Richards A, Mosekilde L. Marked decrease in trabecular bone quality after five years of sodium fluoride therapy--assessed by biomechanical testing of iliac crest bone biopsies in osteoporotic patients. Bone. 1994; 15:393–399. [PubMed: 7917577]
36. Johnsson MS, Nancollas GH. The role of brushite and octacalcium phosphate in apatite formation. Crit Rev Oral Biol Med. 1992; 3:61–82. [PubMed: 1730071]
37. Schilling AF, Linhart W, Filke S, Gebauer M, Schinke T, Rueger JM, Amling M. Resorbability of bone substitute biomaterials by human osteoclasts. Biomaterials. 2004; 25:3963–3972. [PubMed: 15046886]
38. Burg, KJL.; Orr, DE. Degradation rate of bioresorbable materials. Woodhead; Cambridge: 2008.
39. Lin FH, Liao CJ, Chen KS, Sun JS, Liu HC. Degradation behaviour of a new bioceramic: Ca2P2O7 with addition of Na4P2O7.10H2O. Biomaterials. 1997; 18:915–921. [PubMed: 9199761]
40. Silver IA, Murrills RJ, Etherington DJ. Microelectrode studies on the acid microenvironment beneath adherent macrophages and osteoclasts. Exp Cell Res. 1988; 175:266–276. [PubMed: 3360056]
41. Kuemmerle JM, Oberle A, Oechslin C, Bohner M, Frei C, Boecken I, von Rechenberg B. Assessment of the suitability of a new brushite calcium phosphate cement for cranioplasty - an experimental study in sheep. J Craniomaxillofac Surg. 2005; 33:37–44. [PubMed: 15694148]
42. Uskokovic V, Desai TA. Phase composition control of calcium phosphate nanoparticles for tunable drug delivery kinetics and treatment of osteomyelitis. I. Preparation and drug release. J Biomed Mater Res A. 2013; 101:1416–1426. [PubMed: 23115118]
43. Uskokovic V, Hoover C, Vukomanovic M, Uskokovic DP, Desai TA. Osteogenic and antimicrobial nanoparticulate calcium phosphate and poly-(D,L-lactide-co-glycolide) powders for the treatment of osteomyelitis. Mater Sci Eng C Mater Biol Appl. 2013; 33:3362–3373. [PubMed: 23706222]
44. Larsen MJ. An investigation of the theoretical background for the stability of the calcium-phosphate salts and their mutual conversion in aqueous solutions. Arch Oral Biol. 1986; 31:757–761. [PubMed: 3479063]
45. Uskokovic V, Desai TA. Phase composition control of calcium phosphate nanoparticles for tunable drug delivery kinetics and treatment of osteomyelitis. II. Antibacterial and osteoblastic response. J Biomed Mater Res A. 2013; 101:1427–1436. [PubMed: 23115128]
46. Uskokovic V. Revisiting the Fundamentals in the Design and Control of Nanoparticulate Colloids in the Frame of Soft Chemistry. Rev J Chem. 2013; 3:271–303. [PubMed: 24490052]

47. Sun JS, Lin FH, Hung TY, Tsuang YH, Chang WH, Liu HC. The influence of hydroxyapatite particles on osteoclast cell activities. J Biomed Mater Res. 1999; 45:311–321. [PubMed: 10321703]
48. Muller KH, Motskin M, Philpott AJ, Routh AF, Shanahan CM, Duer MJ, Skepper JN. The effect of particle agglomeration on the formation of a surface-connected compartment induced by hydroxyapatite nanoparticles in human monocyte-derived macrophages. Biomaterials. 2014; 35:1074–1088. [PubMed: 24183166]
49. Uskokovic V. The Role of Hydroxyl Channel in Defining Selected Physicochemical Peculiarities Exhibited by Hydroxyapatite. RSC Adv. 2015; 5:36614–36633. [PubMed: 26229593]
50. Parodi JA, Hickok RL, Segelken WG, Cooper JR. Electronic Paramagnetic Resonance Study of the Thermal Decomposition of Dibasic Calcium Orthophosphate. Journal of The Electrochemical Society. 1965; 112:688–692.
51. Bennett RM, Lehr JR, McCarty DJ. Factors affecting the solubility of calcium pyrophosphate dihydrate crystals. J Clin Invest. 1975; 56:1571–1579. [PubMed: 423]
52. Nancollas GH, Marshall RW. Kinetics of dissolution of dicalcium phosphate dihydrate crystals. J Dent Res. 1971; 50:1268–1272. [PubMed: 5285786]
53. Combes C, Rey C. Amorphous calcium phosphates: synthesis, properties and uses in biomaterials. Acta Biomater. 2010; 6:3362–3378. [PubMed: 20167295]
54. McDowell H, Gregory TM, Brown WE. Solubility of Ca//5(PO//4)//3OH in the system Ca(OH)//2-H//3PO//4-H//2O at 5, 15, 25 and 37 degree C. J Res Natl Bur Stand Sect A Phys Chem. 1977; 81:273–281.
55. Coudert AE, Del Fattore A, Baulard C, Olaso R, Schiltz C, Collet C, Teti A, de Vernejoul MC. Differentially expressed genes in autosomal dominant osteopetrosis type II osteoclasts reveal known and novel pathways for osteoclast biology. Lab Invest. 2014; 94:275–285. [PubMed: 24336069]
56. Kokubo T, Kushitani H, Sakka S, Kitsugi T, Yamamuro T. Solutions able to reproduce in vivo surface-structure changes in bioactive glass-ceramic A-W. J Biomed Mater Res. 1990; 24:721–734. [PubMed: 2361964]
57. Rohanová D, Boccaccini AR, Horkavcová D, Bozděchová P, Bezdička P, Častorálová M. Is non-buffered DMEM solution a suitable medium for in vitro bioactivity tests? J Mater Chem B. 2014; 2:5068–5076.
58. Tas CA. X-ray-amorphous calcium phosphate (ACP) synthesis in a simple biomineralization medium. J Mater Chem B. 2013; 1:4511–4520.
59. Montazerolghaem M, Karlsson Ott M, Engqvist H, Melhus H, Rasmusson AJ. Resorption of monetite calcium phosphate cement by mouse bone marrow derived osteoclasts. Mater Sci Eng C Mater Biol Appl. 2015; 52:212–218. [PubMed: 25953560]
60. Francis MD, Slough CL, Briner WW, Oertel RP. An in vitro and in vivo investigation of mellitate and ethane-1-hydroxy-1,1-diphosphonate in calcium phosphate systems. Calcif Tissue Res. 1977; 23:53–60. [PubMed: 19135]
61. Ono K, Wada S. Regulation of calcification by bisphosphonates. Clin Calcium. 2004; 14:60–63. [PubMed: 15577056]
62. Fleisch H, Bisaz S. Mechanism of calcification: inhibitory role of pyrophosphate. Nature. 1962; 195:911. [PubMed: 13893487]
63. Villa-Bellosta R, Sorribas V. Calcium phosphate deposition with normal phosphate concentration. - Role of pyrophosphate. Circ J. 2011; 75:2705–2710. [PubMed: 21799271]
64. Balic Z, Christoffersen MR, Christoffersen J. Structure of the beta form of calcium pyrophosphate tetrahydrate. Acta Crystallogr B. 2000; 56(Pt 6):953–958. [PubMed: 11099960]
65. Gras P, Ratel-Ramond N, Teychene S, Rey C, Elkaim E, Biscans B, Sarda S, Combes C. Structure of the calcium pyrophosphate monohydrate phase (Ca2P2O7.H2O): towards understanding the dehydration process in calcium pyrophosphate hydrates. Acta Crystallogr C Struct Chem. 2014; 70:862–866. [PubMed: 25186358]
66. Zio'l·kowski J. New relation between ionic radii, bond length, and bond strength. Journal of Solid State Chemistry. 1985; 57:269–290.
67. Webb NC. The Crystal Structure of β-Ca2P207. Acta Crystallogr B. 1966; 21:942–948.

68. Pritzker, KPH. Calcium Pyrophosphate Crystal Formation and Dissolution. 1998.
69. Shinozaki T, Pritzker KP. Regulation of alkaline phosphatase: implications for calcium pyrophosphate dihydrate crystal dissolution and other alkaline phosphatase functions. J Rheumatol. 1996; 23:677–683. [PubMed: 8730126]
70. Finckh A, McCarthy GM, Madigan A, Van Linthoudt D, Weber M, Neto D, Rappoport G, Blumhardt S, Kyburz D, Guerne PA. Methotrexate in chronic-recurrent calcium pyrophosphate deposition disease: no significant effect in a randomized crossover trial. Arthritis Res Ther. 2014; 16:458. [PubMed: 25315665]
71. Francis MD, Russell RG, Fleisch H. Diphosphonates inhibit formation of calcium phosphate crystals in vitro and pathological calcification in vivo. Science. 1969; 165:1264–1266. [PubMed: 4308521]
72. Leu CT, Luegmayr E, Freedman LP, Rodan GA, Reszka AA. Relative binding affinities of bisphosphonates for human bone and relationship to antiresorptive efficacy. Bone. 2006; 38:628–636. [PubMed: 16185944]
73. Miyamoto T, Suda T. Differentiation and function of osteoclasts. Keio J Med. 2003; 52:1–7. [PubMed: 12713016]
74. Alfrey AC, Solomons CC, Ciricillo J, Miller NL. Extraosseous calcification. Evidence for abnormal pyrophosphate metabolism in uremia. J Clin Invest. 1976; 57:692–699. [PubMed: 175091]
75. Hsu YC, Chang CW, Lin CL, Lai CT. Calcium pyrophosphate dihydrate deposition disease of the spleen. Am J Surg. 2010; 200:e28–29. [PubMed: 20538255]
76. Chen KH, Li MJ, Cheng WT, Balic-Zunic T, Lin SY. Identification of monoclinic calcium pyrophosphate dihydrate and hydroxyapatite in human sclera using Raman microspectroscopy. Int J Exp Pathol. 2009; 90:74–78. [PubMed: 19200254]
77. Jung A, Bisaz S, Fleisch H. The binding of pyrophosphate and two diphosphonates by hydroxyapatite crystals. Calcif Tissue Res. 1973; 11:269–280. [PubMed: 4350498]
78. Kuo YJ, Tsuang FY, Sun JS, Lin CH, Chen CH, Li JY, Huang YC, Chen WY, Yeh CB, Shyu JF. Calcitonin inhibits SDCP-induced osteoclast apoptosis and increases its efficacy in a rat model of osteoporosis. PLoS One. 2012; 7:e40272. [PubMed: 22792258]
79. Lin K, Yuan W, Wang L, Lu J, Chen L, Wang Z, Chang J. Evaluation of host inflammatory responses of beta-tricalcium phosphate bioceramics caused by calcium pyrophosphate impurity using a subcutaneous model. J Biomed Mater Res B Appl Biomater. 2011; 99:350–358. [PubMed: 21948342]
80. Mikhael MM, Chioffe MA, Shapiro GS. Calcium pyrophosphate dihydrate crystal deposition disease (pseudogout) of lumbar spine mimicking osteomyelitis-discitis with epidural phlegmon. Am J Orthop (Belle Mead NJ). 2013; 42:E64–67. [PubMed: 24078961]
81. Pang L, Hayes CP, Buac K, Yoo DG, Rada B. Pseudogout-associated inflammatory calcium pyrophosphate dihydrate microcrystals induce formation of neutrophil extracellular traps. J Immunol. 2013; 190:6488–6500. [PubMed: 23677474]
82. Sommer B, Felix R, Sprecher C, Leunig M, Ganz R, Hofstetter W. Wear particles and surface topographies are modulators of osteoclastogenesis in vitro. J Biomed Mater Res A. 2005; 72:67–76. [PubMed: 15536650]
83. Schilling AF, Filke S, Brink S, Korbmacher H, Amling M, Rueger JM. Osteoclasts and biomaterials. Eur J Trauma. 2006; 32:107–113.
84. Allori AC, Sailon AM, Warren SM. Biological basis of bone formation, remodeling, and repair-part I: biochemical signaling molecules. Tissue Eng Part B Rev. 2008; 14:259–273. [PubMed: 18665803]
85. Keller J, Brink S, Busse B, Schilling AF, Schinke T, Amling M, Lange T. Divergent resorbability and effects on osteoclast formation of commonly used bone substitutes in a human in vitro-assay. PLoS One. 2012; 7:e46757. [PubMed: 23071629]
86. Detsch R, Mayr H, Ziegler G. Formation of osteoclast-like cells on HA and TCP ceramics. Acta Biomater. 2008; 4:139–148. [PubMed: 17723325]
87. Boyde A, Ali NN, Jones SJ. Resorption of dentine by isolated osteoclasts in vitro. Br Dent J. 1984; 156:216–220. [PubMed: 6584143]

88. Yamada S, Heymann D, Bouler JM, Daculsi G. Osteoclastic resorption of calcium phosphate ceramics with different hydroxyapatite/beta-tricalcium phosphate ratios. Biomaterials. 1997; 18:1037–1041. [PubMed: 9239465]

89. Xia Z, Grover LM, Huang Y, Adamopoulos IE, Gbureck U, Triffitt JT, Shelton RM, Barralet JE. In vitro biodegradation of three brushite calcium phosphate cements by a macrophage cell-line. Biomaterials. 2006; 27:4557–4565. [PubMed: 16720039]

90. Ishikawa K. Bone substitute fabrication based on dissolution-precipitation reactions. Materials. 2010; 3:1138–1155.

Highlights

- Solubility of Ca orthophosphates is the determinant of osteoclastic resorbability.
- DCP > ACP > HAP trend in solubility remained in effect in the osteoclastic culture.
- Dissolution of Ca pyrophosphate was obstructed following the particle uptake.
- Combination of different CAPs may be most beneficial for optimal resorption.

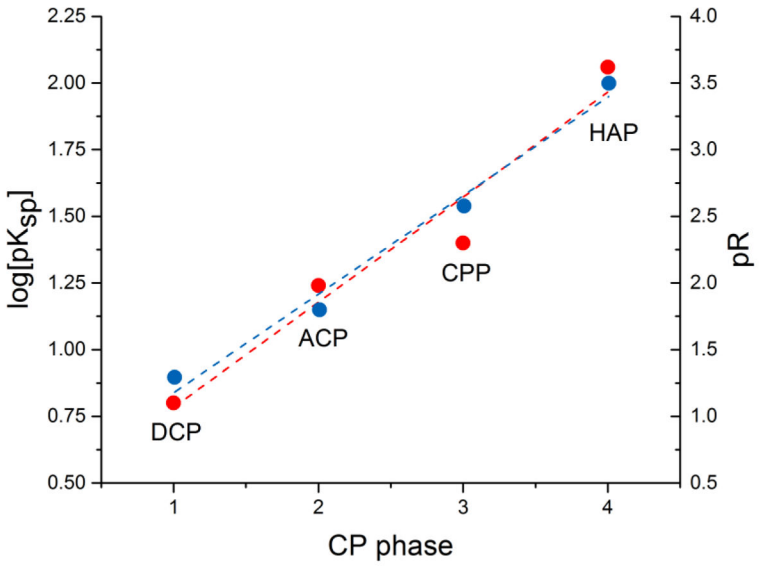

Fig. 1.

Linear fit of the negative logarithmic values of logK_{sp} (●, ---) and absolute solubilities (R) (●, ---) as a function of the number of four different CP powders utilized: DCP, ACP, CPP and HAP.

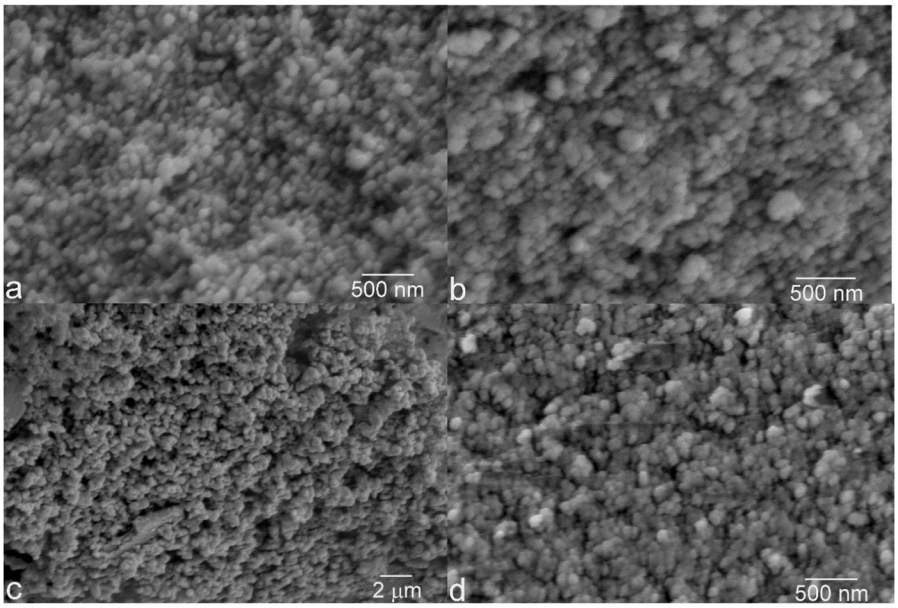

Fig. 2.

Scanning electron micrographs of four different CP powders synthesized: DCP (a), ACP (b), CPP (c), and HAP (d).

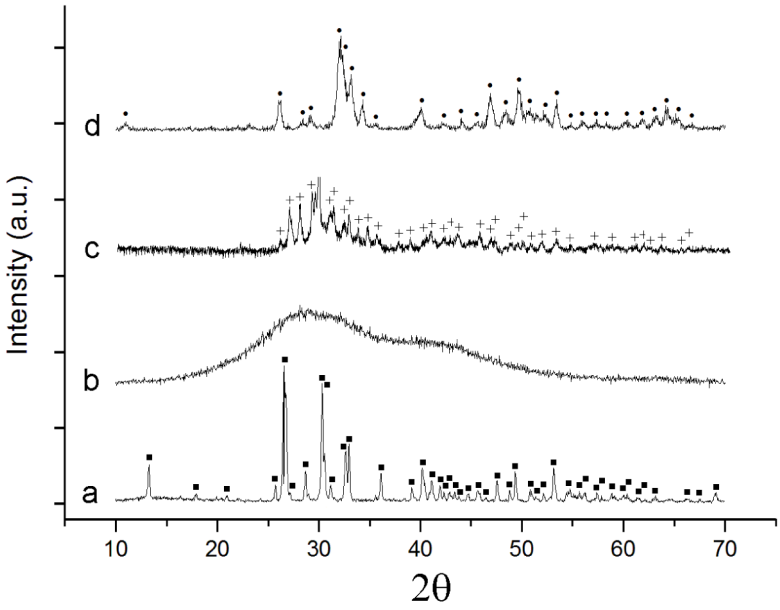

Fig. 3.

X-ray diffractograms of four different monophasic CP powders synthesized: DCP (a), ACP (b), CPP (c), and HAP (d). Crystallographic planes corresponding to the given phases are labeled with the following symbols: DCP – ■; HAP - ●; CPP - +.

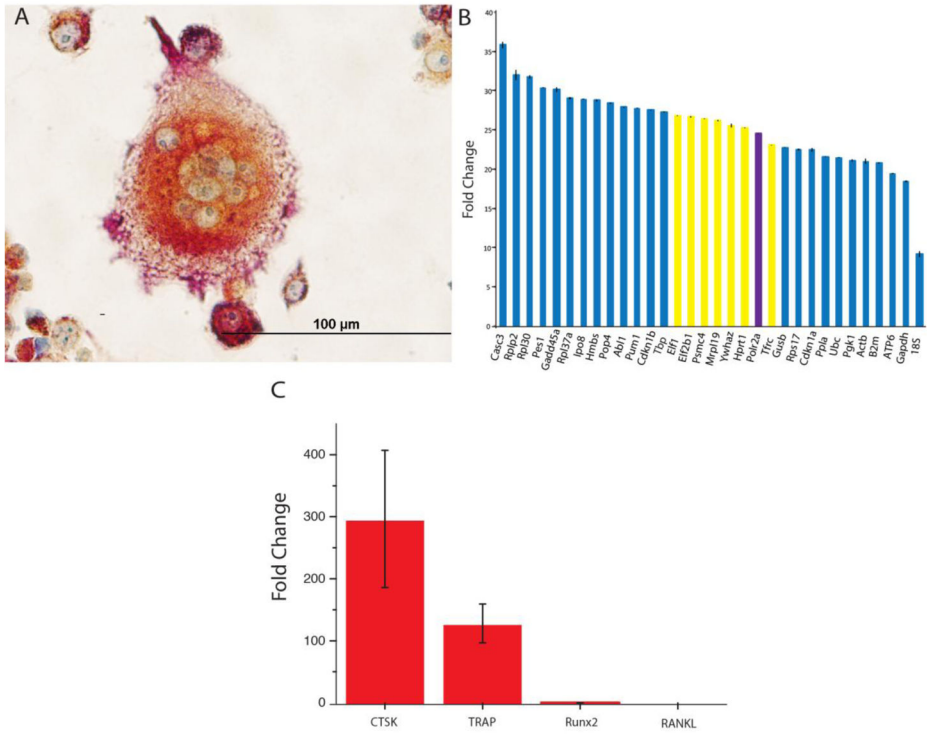

Fig. 4.

A Bright-field optical image of TRAP-stained RAW264.7 cells differentiated into an osteoclastic lineage using mRANKL (A). An array of housekeeping genes analyzed for expression in RAW264.7 cells using real-time PCR and arranged from left to right in the order of an increase in their expression (B). Highlighted in yellow are genes falling between C_t of 23 and 27 and being the most optimal for use as internal controls, while highlighted in purple is the one chosen for that role in this study: POLR2A, peaking at $C_t = 24.485$ and having the lowest standard deviation for n = 3 among all the 8 genes with $23 < C_t < 27$: 0.046. Gene regulation of the activity of osteoclastic markers *CTSK* and *TRAP* and osteoblastic markers *Runx2* and *RANKL* quantified using real-time PCR and normalized to the expression of the housekeeping gene POLR2A (C).

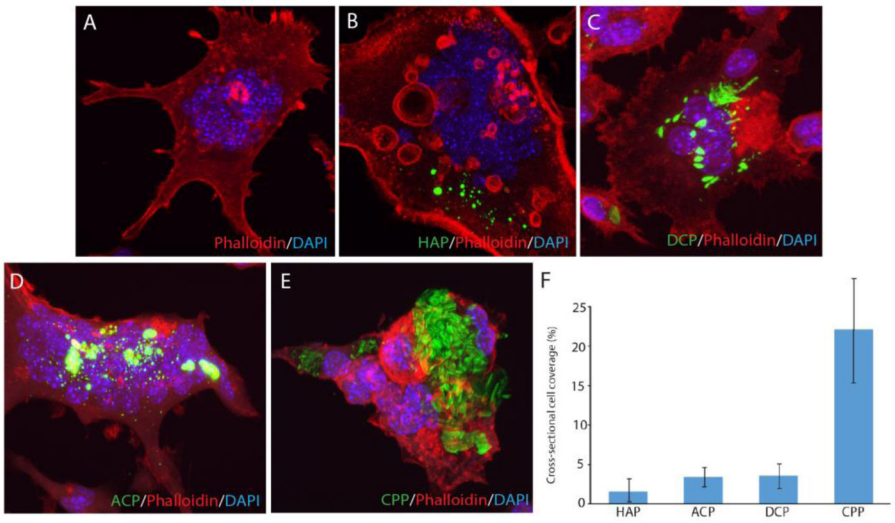

Fig. 5.

Confocal optical images of RAW264.7 cells incubated either with no CP particles (a) or with the identical amounts of different CP particles (HAP, DCP, ACP, CPP) for 7 days (b–e) and the comparison of the cross-sectional surface coverage of their cytoplasmic interiors after the same period of time (f). Data are shown as averages with error bars representing standard deviation.

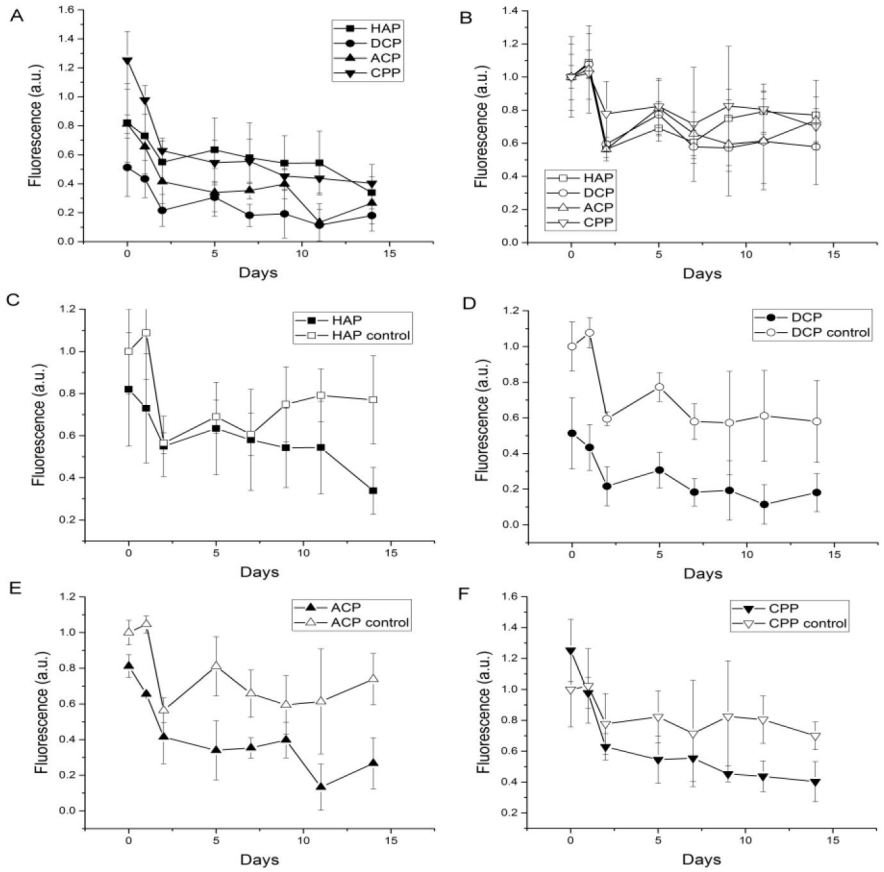

Fig. 6.

Degradation of CP powders with (full symbols) and without (empty symbols) the osteoclastic RAW264.7 cells assessed by measuring a change in the fluorescence of the OsteoImage™ fluorophore adsorbed on the surface of CP particles kept in cell culture for 14 days. Data are shown as averages with error bars representing standard deviation.

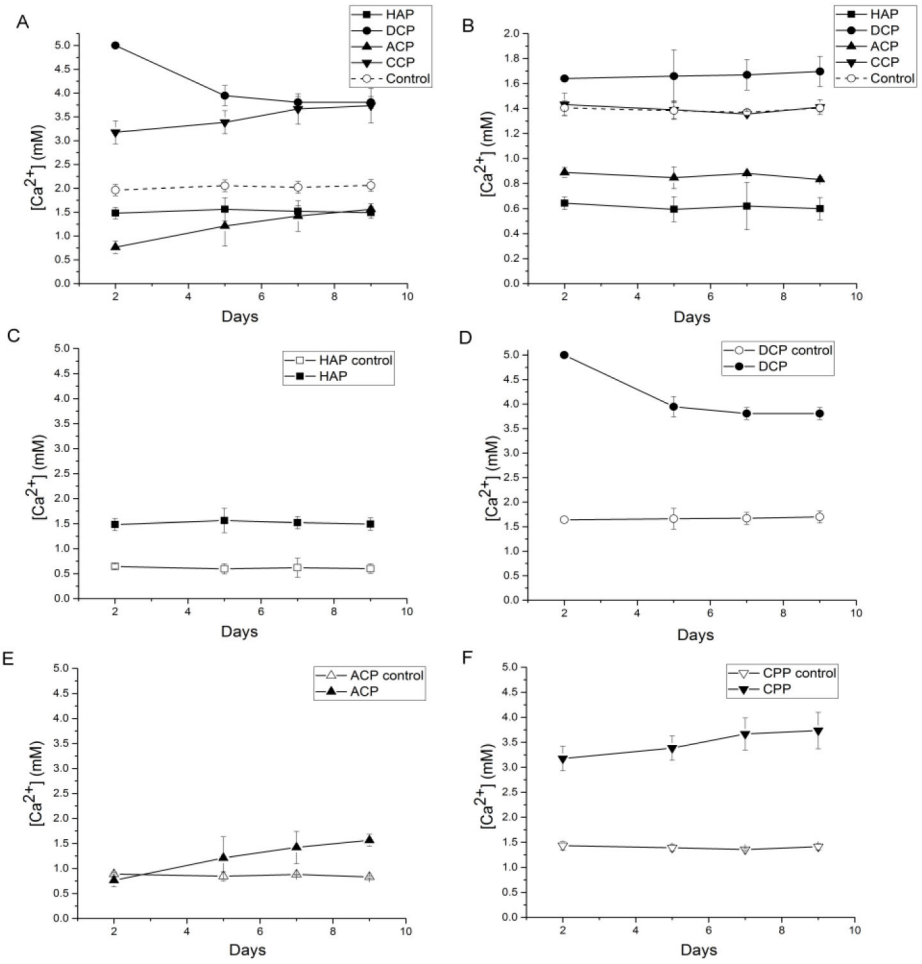

Fig. 7.

Free Ca^{2+} concentrations in the cell culture medium supernatants during the incubation with different CP powders, with (a) and without (b) the osteoclastic RAW264.7 cells. Comparison between free Ca^{2+} concentrations for each of the four different CP powders with (full symbols) and without (empty symbols) the osteoclastic RAW264.7 cells on the scale of 0 – 5 mM are shown in (c) – (f). Data are shown as averages with error bars representing standard deviation.

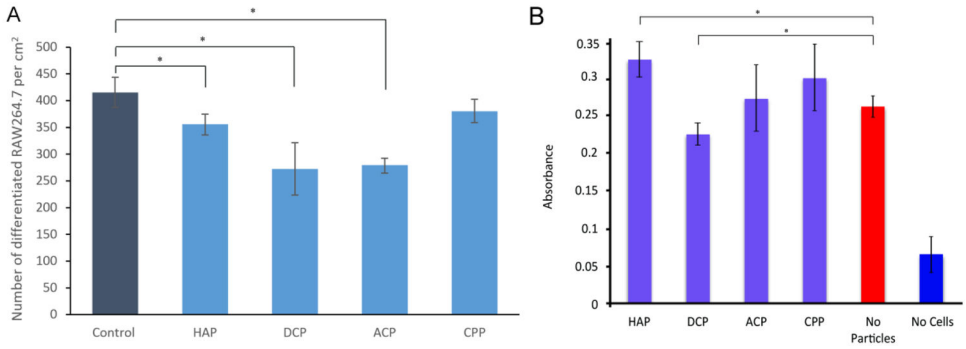

Fig. 8.

The number of differentiated RAW264.7 cells per surface area in the presence of different CP powders (A) and MTT assay absorbance, indicative of cell viability, for differentiated, osteoclast-like RAW264.7 cells incubated with various CP powders at the concentration of 2.6 mg/cm^2 (5 mg per well in a standard 24 well plate) (B). Data normalized to the viability of the control sample are shown as averages with error bars representing standard deviation. Samples for which a statistically significant difference ($p < 0.05$) was observed when compared to the control are denoted with *.

Table 1

CP phases synthesized as a part of this study and arranged in the order of their solubility: dicalcium phosphate anhydrous (DCP), β-calcium pyrophosphate (CPP), amorphous calcium phosphate (ACP) and hydroxyapatite (HAP). Solubility products and solubility values in pure water (pH 7.0) at 25 °C are empirical in origin and obtained from Refs. [51] (DCP), [52] (CPP), [53] (ACP), and [54] (HAP).

Phase	Chemical formula	Space group	pK_{sp}	Solubility (g/dm^3)
DCP	$CaHPO_4$	Triclinic $P^{\bar{1}}$	7.0	4.8×10^{-2}
CPP	$Ca_2P_2O_7$	Tetragonal $P4_1$	18.5	1.5×10^{-2}
ACP	$Ca_3(PO_4)_2 \cdot nH_2O$	/	25	2.5×10^{-3}
HAP	$Ca_5(PO_4)_3OH$	Hexagonal $P6_3/m$	58.5	3×10^{-4}